

Summary:
**Innovative Confinement Concepts,
Operational Scenarios and Confinement**
23rd IAEA Fusion Energy Conference

R. J. Hawryluk

October 16, 2010

Acknowledgments to:

**E. Belova, D. Gates, T. S. Hahm, S. Kaye, C. Kessel, R. Maingi,
G. H. Neilson, S. Prager, W. Solomon and M. Zarnstorff**

Outline

<i>Topical Area:</i>	<i>Number of Papers</i>
Innovative Confinement Concepts	10
Operational Scenarios	28
– Stellarators	
– Elmy H-modes	
– Advanced Operating Modes	
Confinement Experiments	51
– Energy Transport and Turbulence	
– Particle Transport	
– Rotation and Momentum Transport	
– L-H transition and Pedestal	

Innovative Confinement Concepts

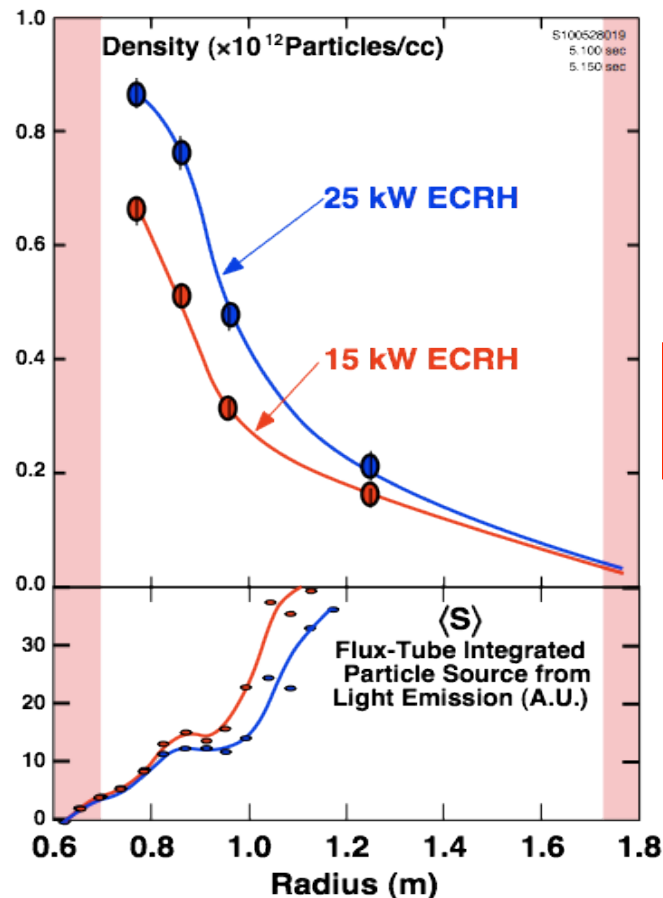
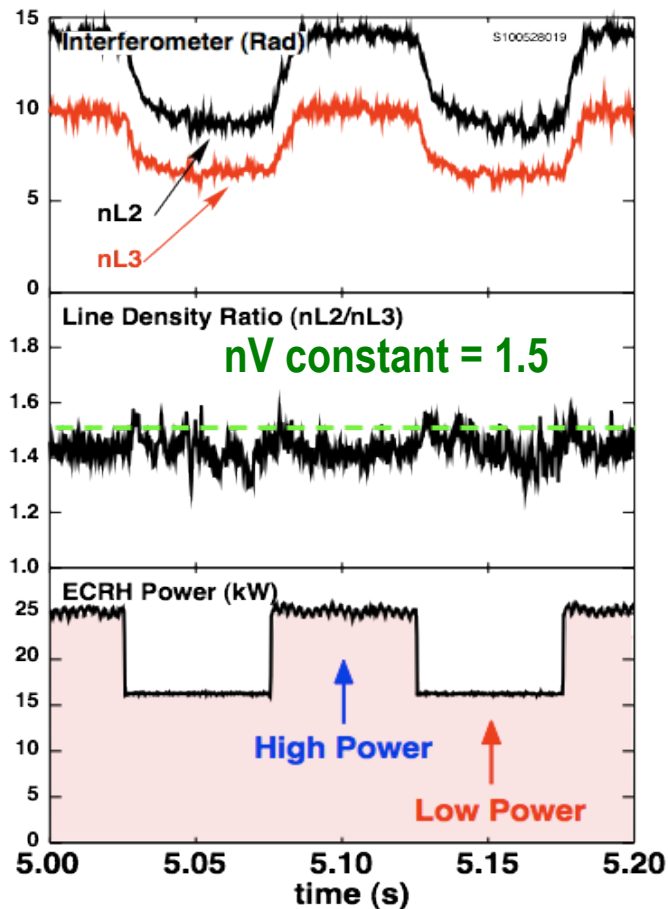
Stimulate New Ideas

Address a broad range of configurations and topics:

- ✓ *Levitated Dipole*
- ✓ *Field Reversed Configuration*
- ✓ *Mirror machines*
- Spheromaks
- Helical-tokamak hybrid
- Magneto-inertial fusion
- Direct energy conversion

Levitated Dipoles (LDX and RT-1) Demonstrate Inward Turbulent Pinch and Validates Flux Expansion Concept

Profile shape remains unchanged near $nV=\text{constant}$ while source term is modulated.



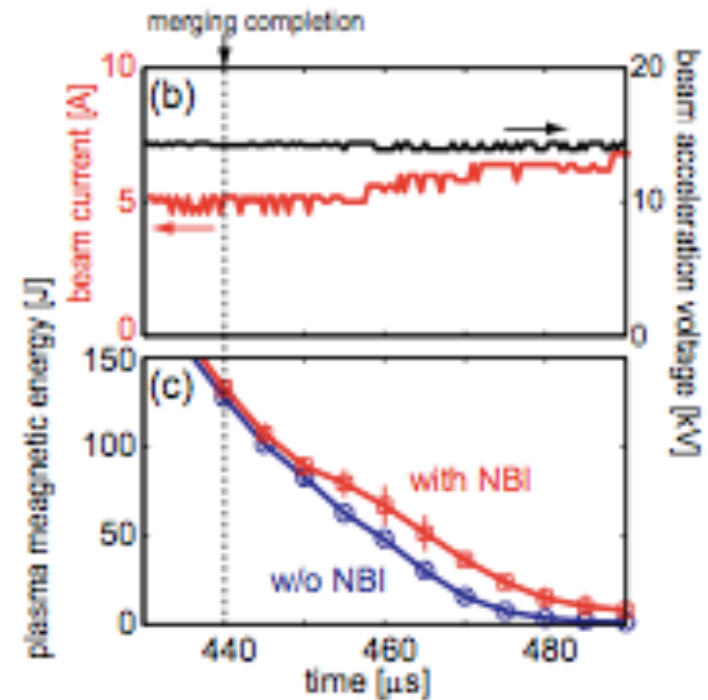
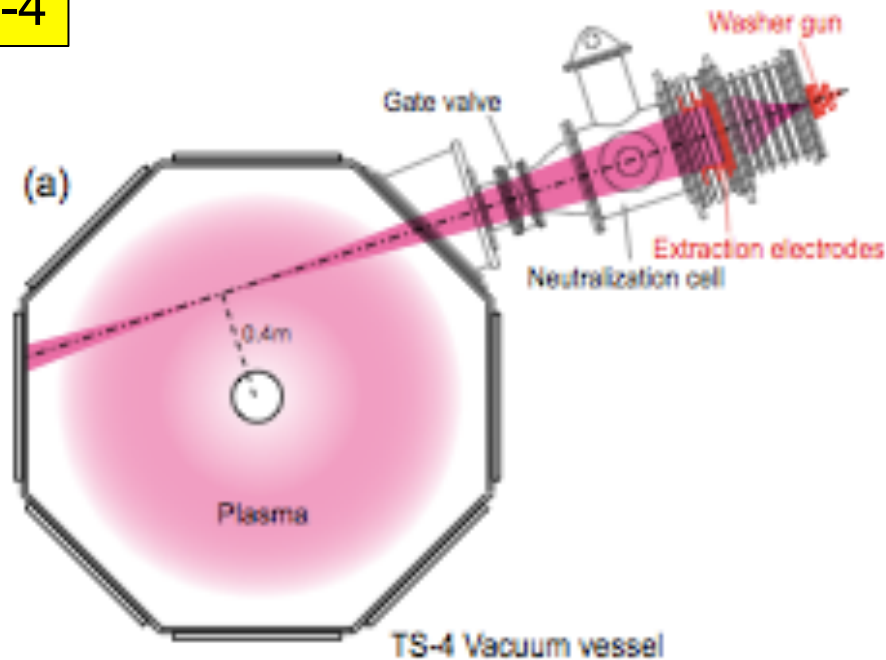
LDX

D. T. Garnier,
ICC/1-1ra

Error field optimized RT-1 plasma achieved peak 70% beta (H. Saitoh, EXC/9-4b).

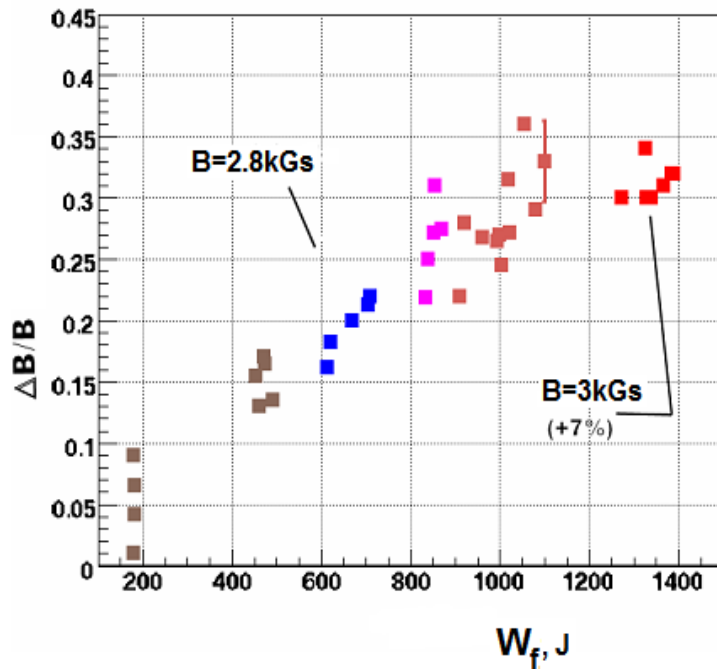
FRC Decay Time Increased by Neutral Beam Injection Suggesting MHD Stabilization

TS-4



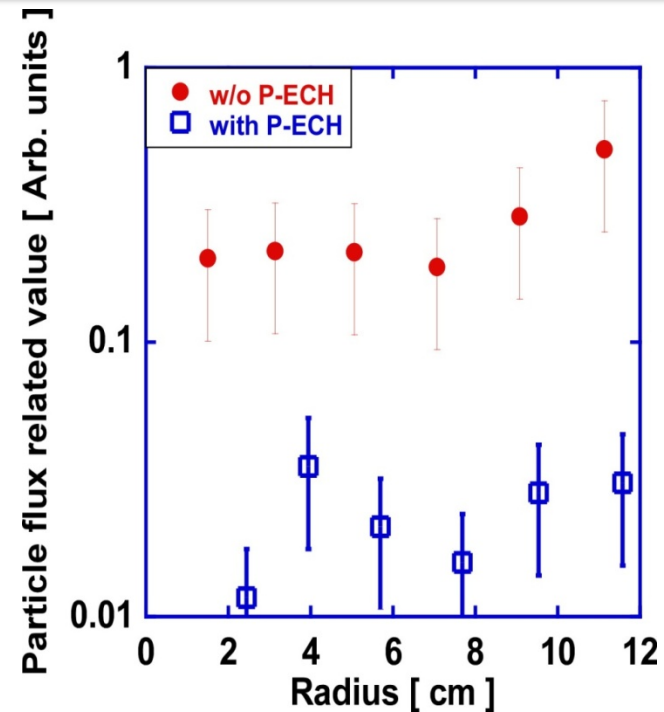
M. Inomoto ICC/P7-01

Increased Heating Power Extended Mirror Machine Performance



E. P. Kruglyakov, OV/P-6

GDT achieved 60% beta and reached ballooning limit



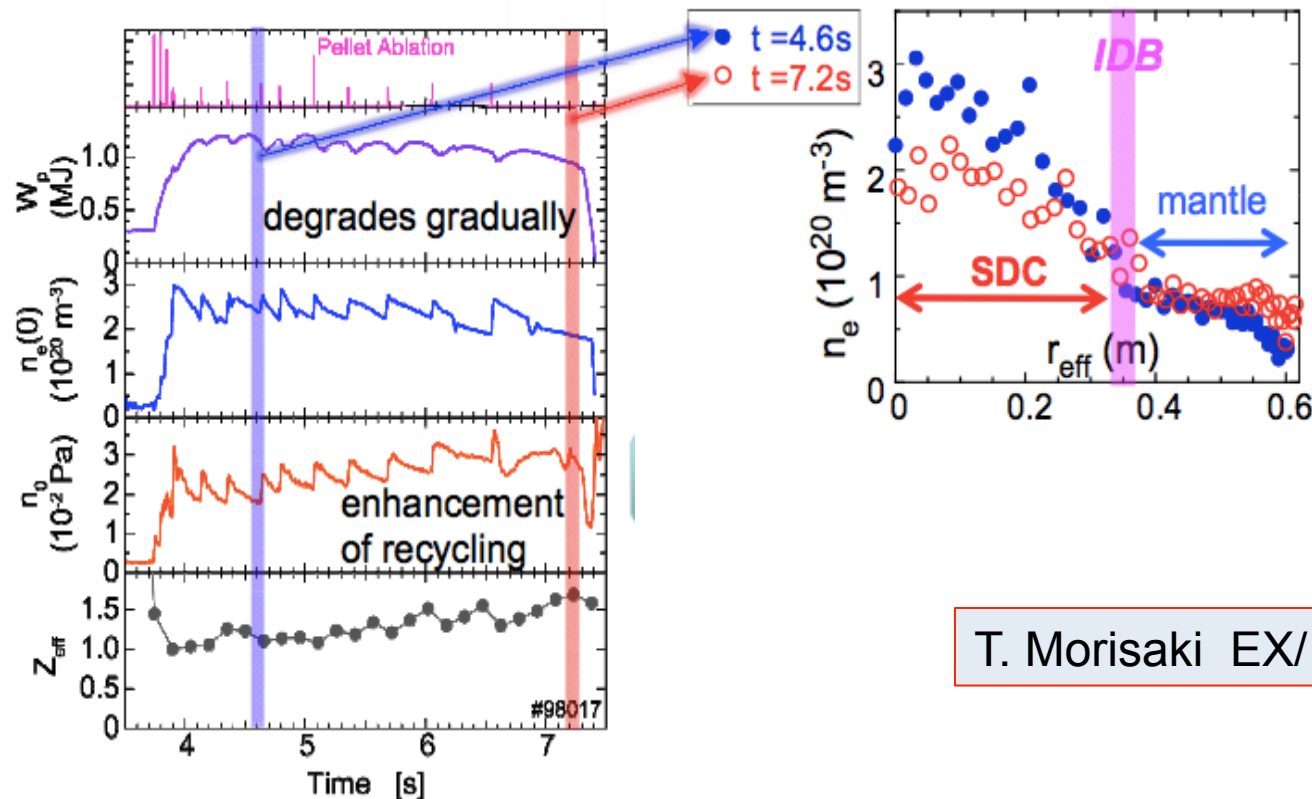
M. Yoshikawa, EXC/P8-21

In Gamma10, ECH reduced fluctuations and inferred radial particle flux.

Outline

<i>Topical Area:</i>	<i>Number of Papers</i>
Innovative Confinement Concepts	10
✓ Operational Scenarios	28
– <i>Stellarators</i>	
– <i>Elmy H-modes</i>	
– <i>Advanced Operating Modes</i>	
Confinement Experiments	51
– Energy Transport and Turbulence	
– Particle Transport	
– Rotation and Momentum Transport	
– L-H transition and Pedestal	

Sustainment of Super-Dense Core by Pellet Injection and Internal Diffusion Barrier in LHD



T. Morisaki EX/1-5

- **Diffusion in edge mantle much greater than in the core.**
 - Enhanced by the application of resonant magnetic field perturbations
- **Impurity accumulation in the core avoided.**
- **LHD has also attained 15keV peak electron temperatures in plasmas with electron ITB (H. Takahashi, EXC/P8-15)**

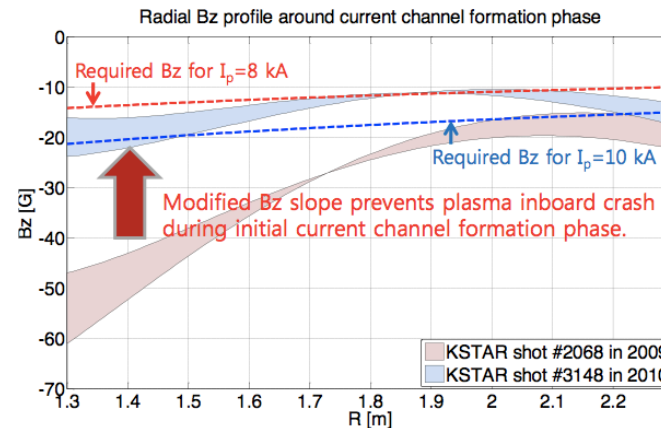
Operational Challenges of Superconducting Tokamaks Successfully Being Met by KSTAR and EAST

EAST

J. Li, OV/1-2



RF Conditioning Antenna



KSTAR

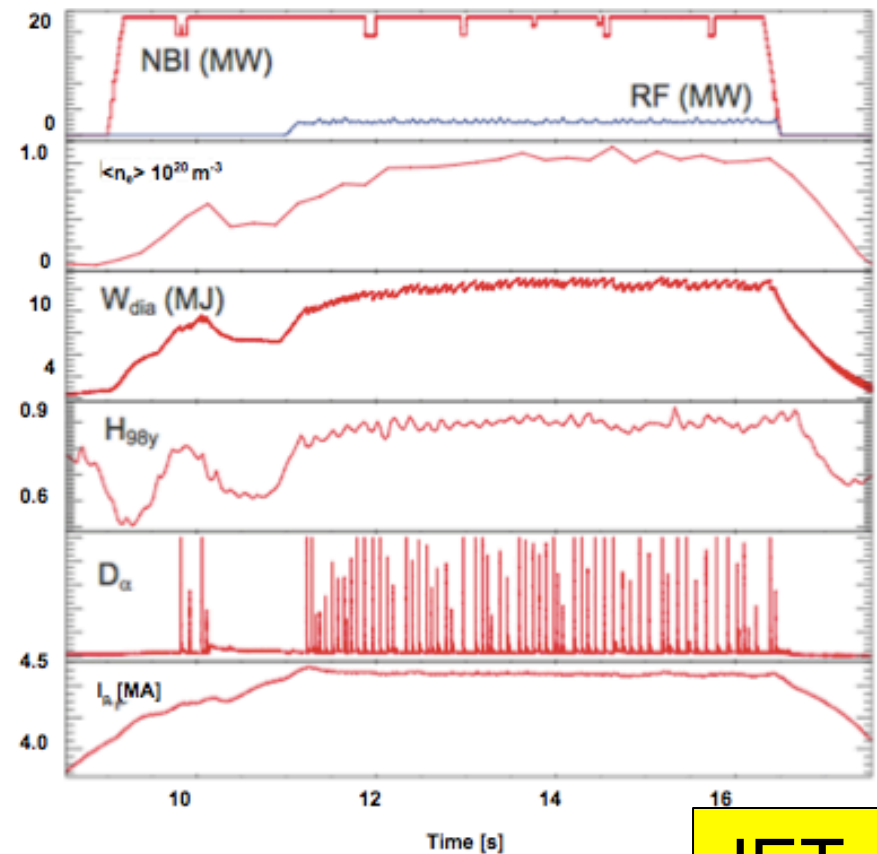
M. Kwon,
OV/1-1

Compensation for ferromagnetic material

- **Wall conditioning: ICRF conditioning, HF GDC, Li Wall Coatings (EAST OV1-2)**
 - Also on Tore Supra (D. Douai, FTP/P1-26)
- **Low voltage startup (0.9MA EAST OV/1-2, 0.5MA KSTAR OV/1-1)**
 - ECH assisted startup (also FTU, A. Tuccillo, OV/4-2)
 - Lower hybrid assisted current ramp (also, E. Marmar, OV/3-2)
- **Magnetic material and eddy current compensation for discharge evolution on KSTAR. (S. W. Yoon, EX/5-1)**

Progress Developing ITER 15MA Startup and Shutdown Scenarios

- JET 4.5MA operation reestablished
- Active ELM moderation required about 3.5MA to prevent carbon ablation.
 - Modest impact on τ_E
- Successful startup and shutdown techniques for ITER demonstrated on JET, DIII-D, and C-Mod
 - See A. C. C. Sips, EXC/P2-08,
J. R. Wilson, EXC/P2-02,
G. L. Jackson, EXS/P2-11

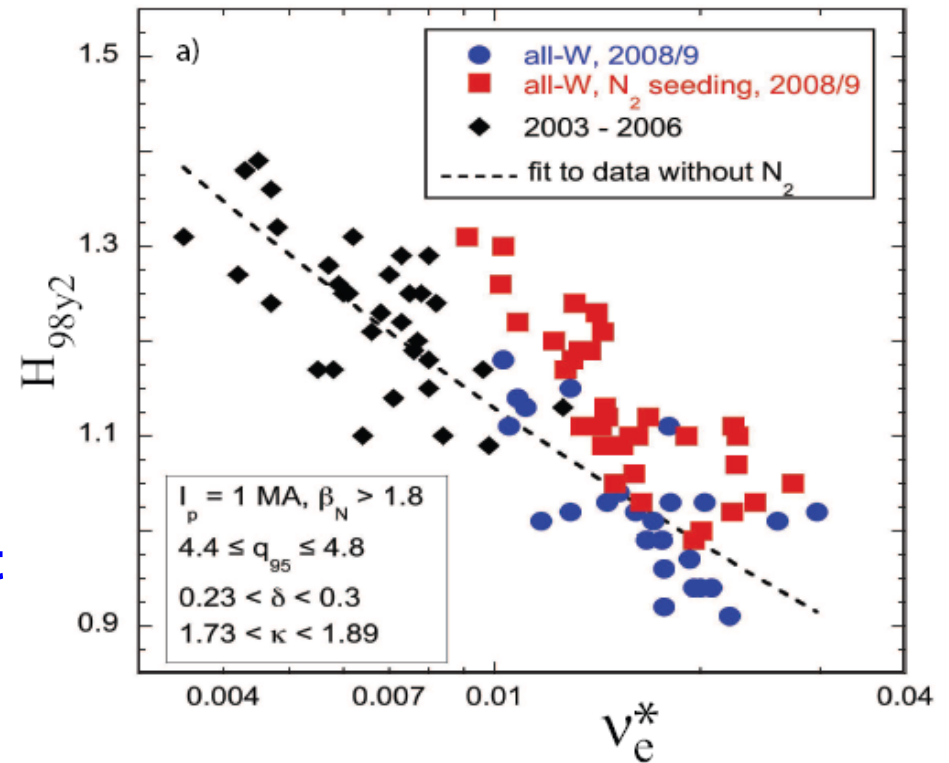


I. Nunes, ECX/P8-03

JET

Impurity Seeding Successfully Reduced Divertor Heat Flux

- **Improvement in τ_E obtained in AUG**
 - Critical for operation with tungsten divertor.
- **JET and C-Mod obtained similar reductions in heat load and operational benefits but did not obtain an improvement in τ_E .**
 - See C. Giroud, EXC/P3-2 and J. Hughes, EXC/P3-6

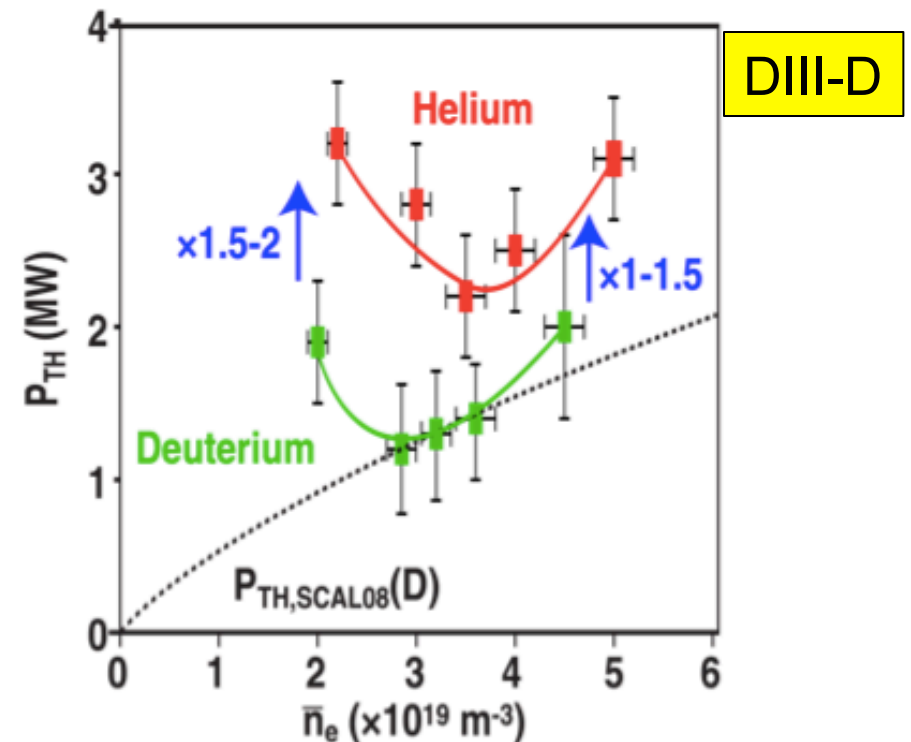


AUG

J. Schweinzer, EXC/P2-07

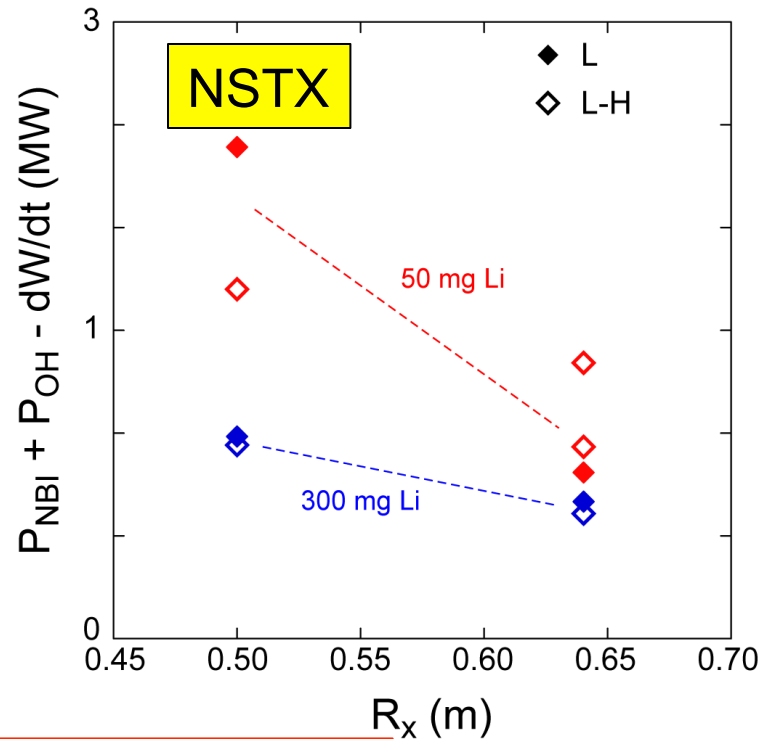
Threshold Power Required for Transition from L to H-mode Has Been Better Characterized for ITER

- P_{LH} compared for He with D for ITER non-nuclear phase:
 - Threshold is density dependent (DIII-D, EXC/2-4Ra and JET, EXC/2-4Rb)
 - In NSTX, P_{LH} is 20 to 40% greater (NSTX, EXC/2-3Rb)
- Low n perturbation increase P_{LH} by 50% (NSTX, EXC/2-3Rb) and 80% (MAST, EXC/2-3Ra)
- P_{LH} significantly increased in DIII-D due to RMP perturbations above a threshold level,
 - Smaller change for non-resonant fields
 - No significant change in DIII-D test blanket simulation. (M. J. Schaffer, ITR/1-3)

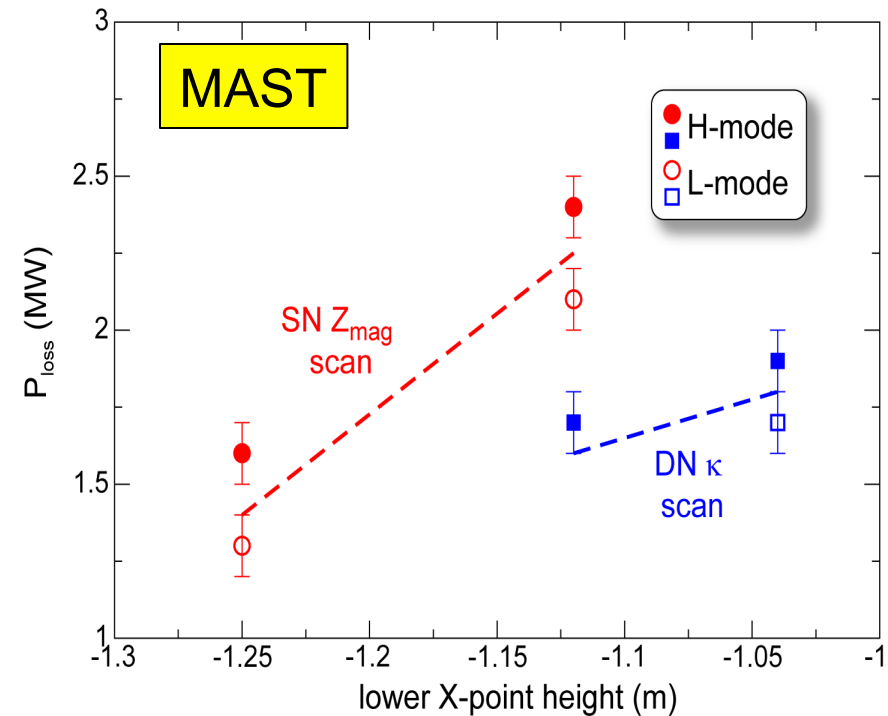


P. Gohil, EXC/2-4Ra

Recycling Conditions Have a Large Impact on L to H Power Threshold



S. Kaye, EXC/2-3Rb



H. Meyer, EXC/2-3Ra

Lithium decreases P_{LH} (NSTX)

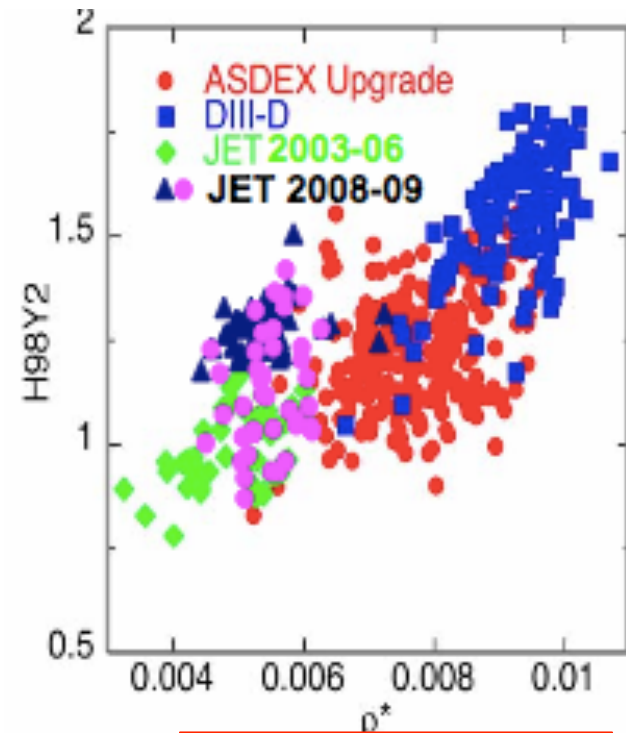
Low triangularity decreases P_{LH} (NSTX)

Depends on height of the x-point (MAST, DIII-D, P. Gohil, EXC/2-4Ra)

Too many hidden variables remain unaccounted for in P_{LH} scaling.

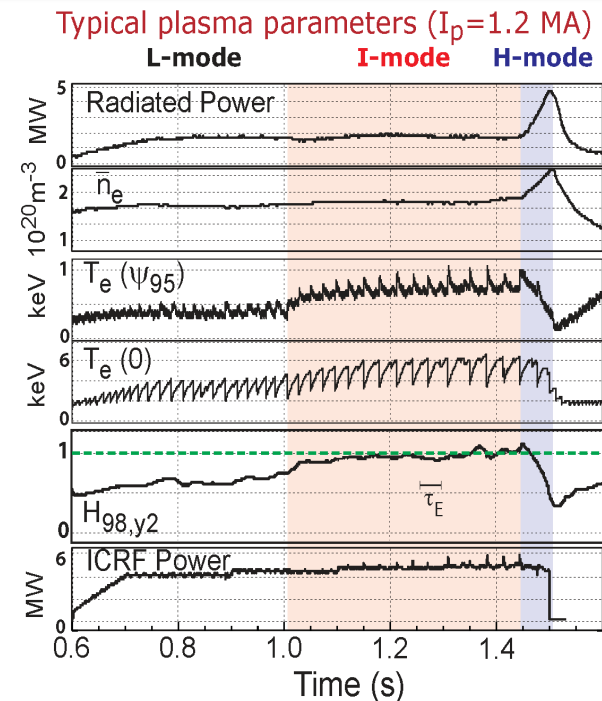
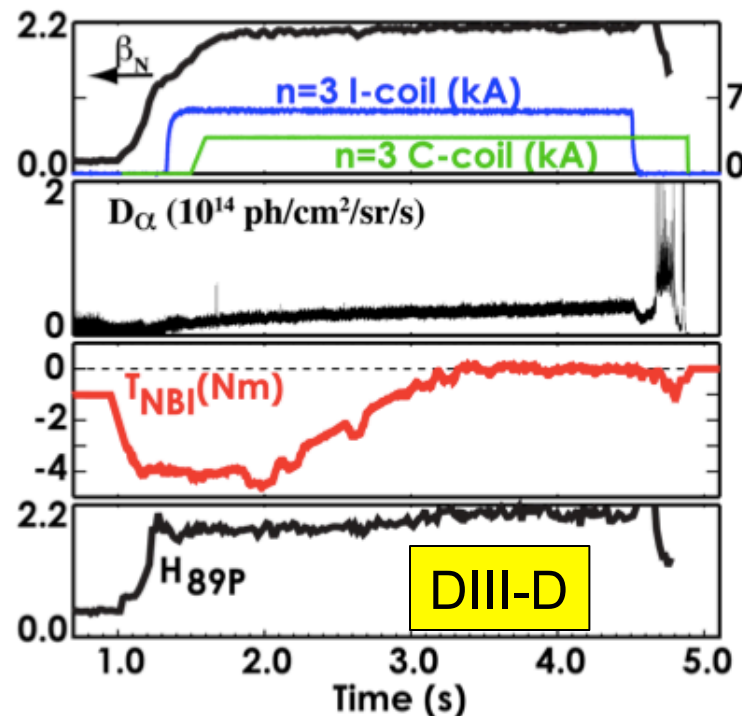
Advanced Inductive Scenarios Are Potentially Attractive Long Duration Discharges in ITER

- Advanced inductive discharges operate at lower current enabling longer duration discharges.
- Recent JET experiments, by ramping the current down prior to main heating phase achieved $H_{98} \sim 1.3$.
 - Significantly improved relative to earlier data.
- Further work is planned on ρ^* and v^* scaling to improve the extrapolation to ITER:
 - Bohm ρ^* scaling between JET and DIII-D
 - Current penetration mechanism



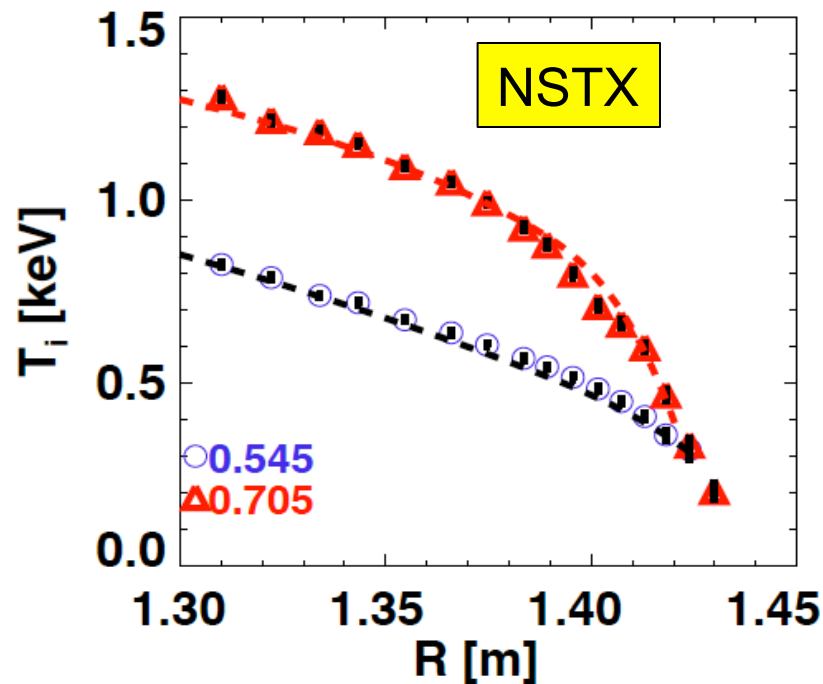
E. Joffrin, EX/1-1
T.C. Luce, ITR/1-5

QH-mode and I-mode Offer the Possibility of ELM Suppressed Operation

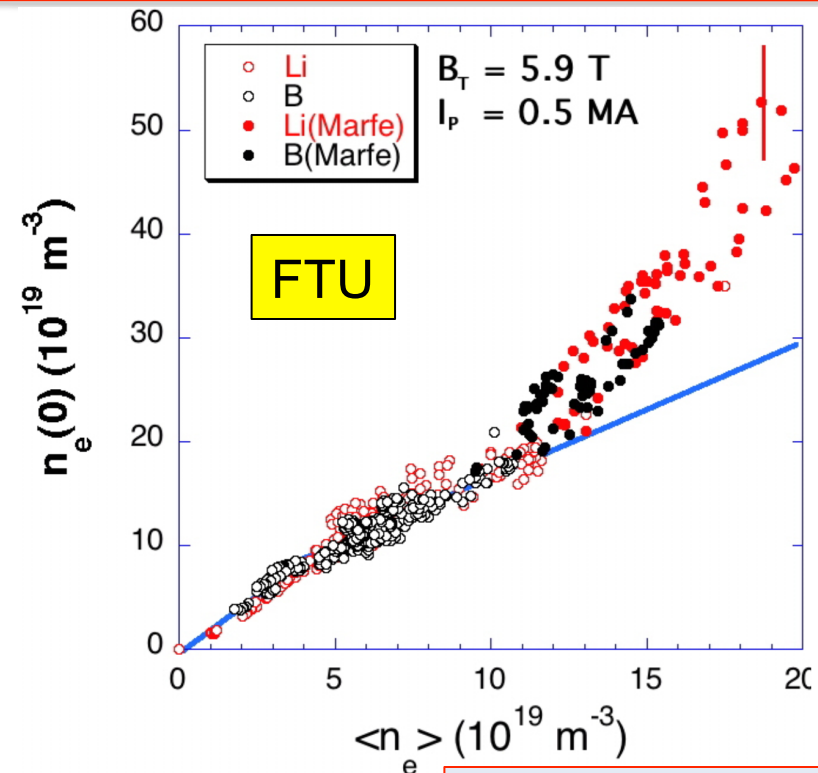


- NTV provides ExB shear to maintain QH-mode even after NBI torque ramped to zero using non-resonant fields. (A. Garofalo, EXS/1-2).
- I-mode usually accessed by operating in unfavorable $B \times \nabla B$ direction (away from active X-point) D. Whyte, EX/1-3
- *Can these scenarios be used on ITER?*

Lithium Improves Energy Confinement and Widens the Operating Window in a Number of Devices



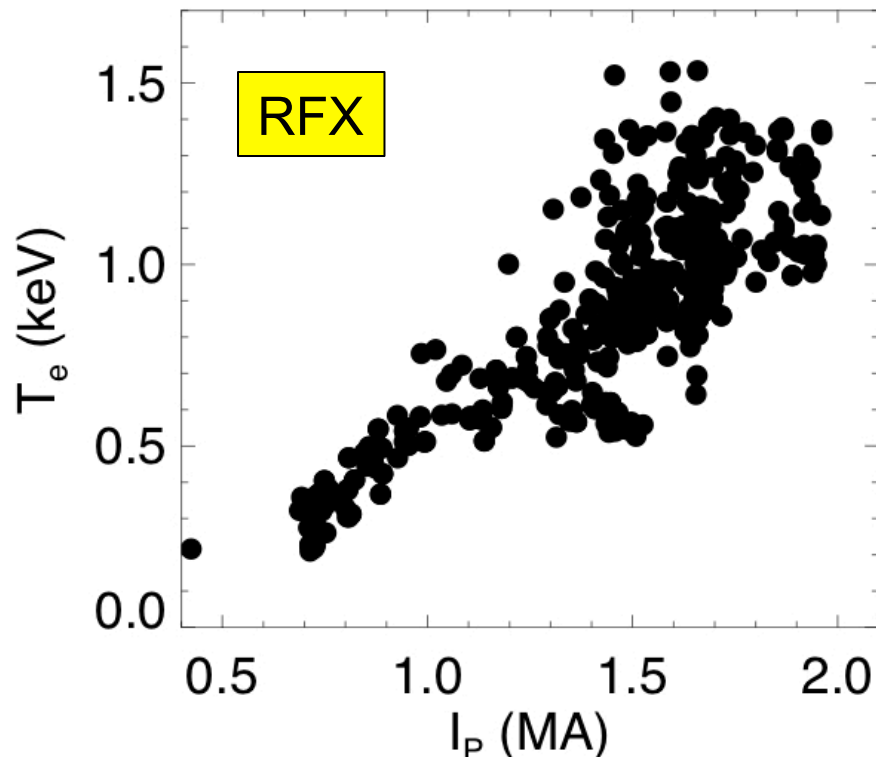
R. Maingi, EXC/2-2



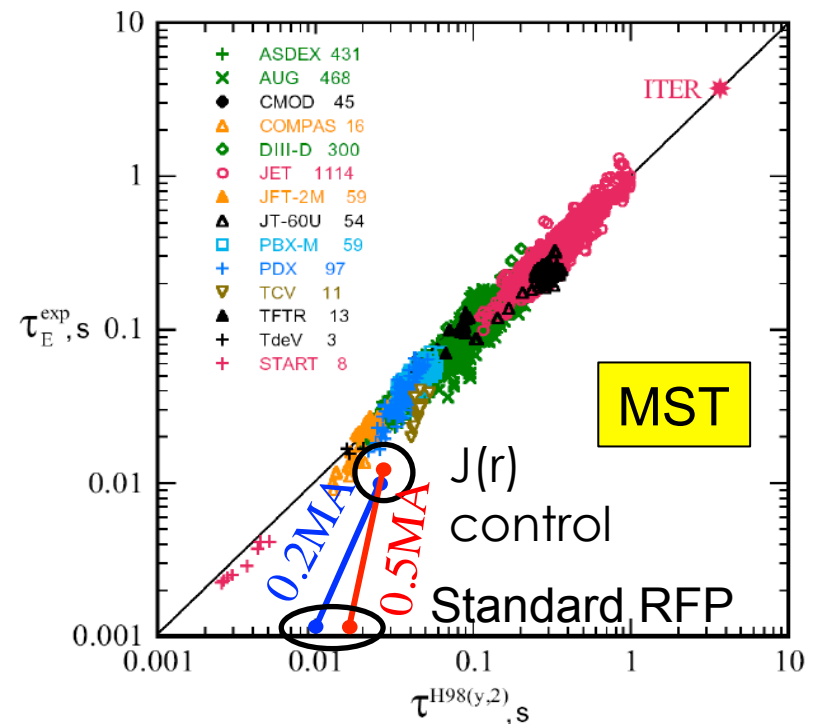
G. Mazzitelli, EXC/6-3

- **FTU, NSTX and TJ-II have obtained up to ~50% τ_E enhancements**
 - FTU obtained peaked profiles with n_e up to $\sim 1.6 n_e^{\text{GW}}$ at high q .
 - TJ-II obtained more peaked density profiles
 - NSTX combined lithium with EP H-mode to achieve $H_{98} \sim 1.8$

RFX and MST Have Extended Their Operating Regimes



P. Martin, OV/5-3Ra



B. Chapman, EXC/P5-01

RFX observed linear increase in T_e with I_p .

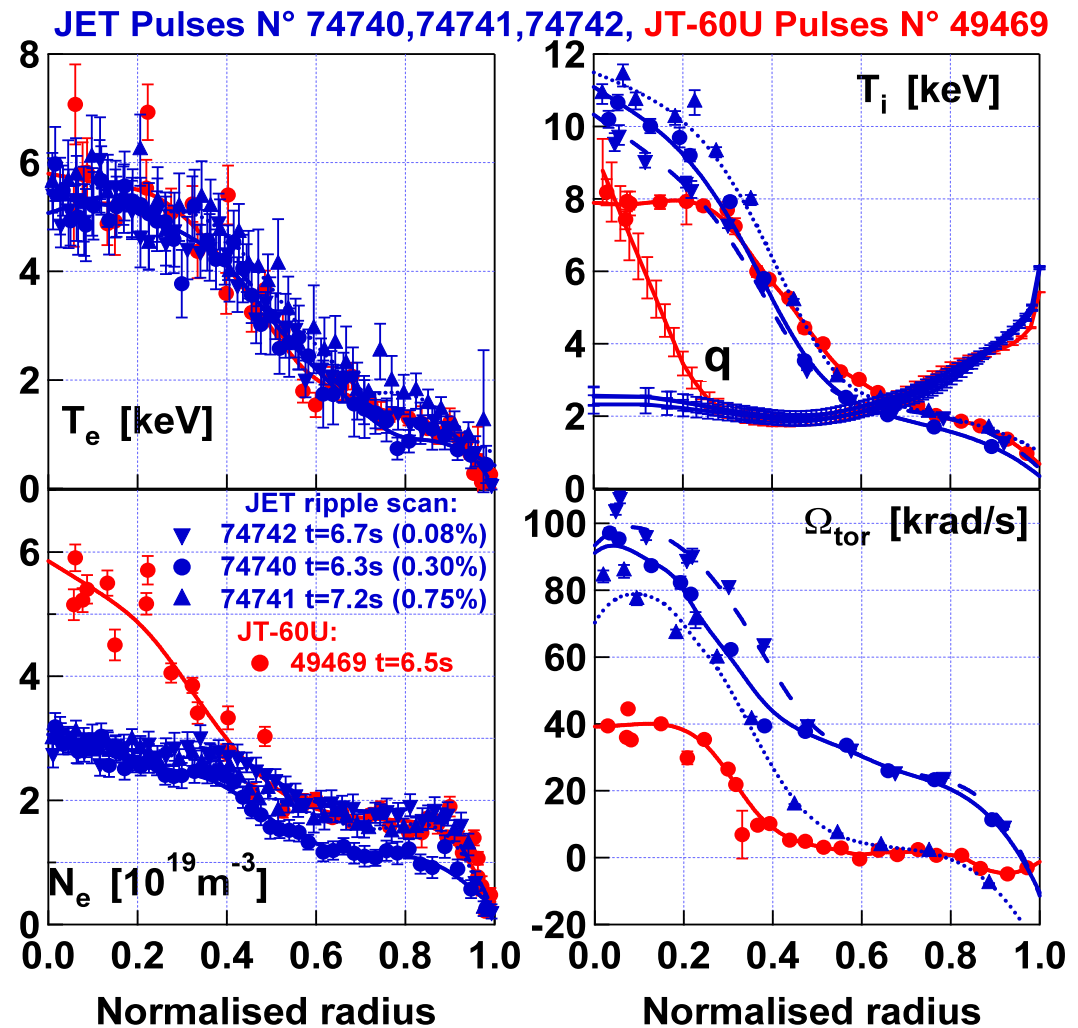
MST attained $\tau_E = 12$ ms by current profile control

Outline

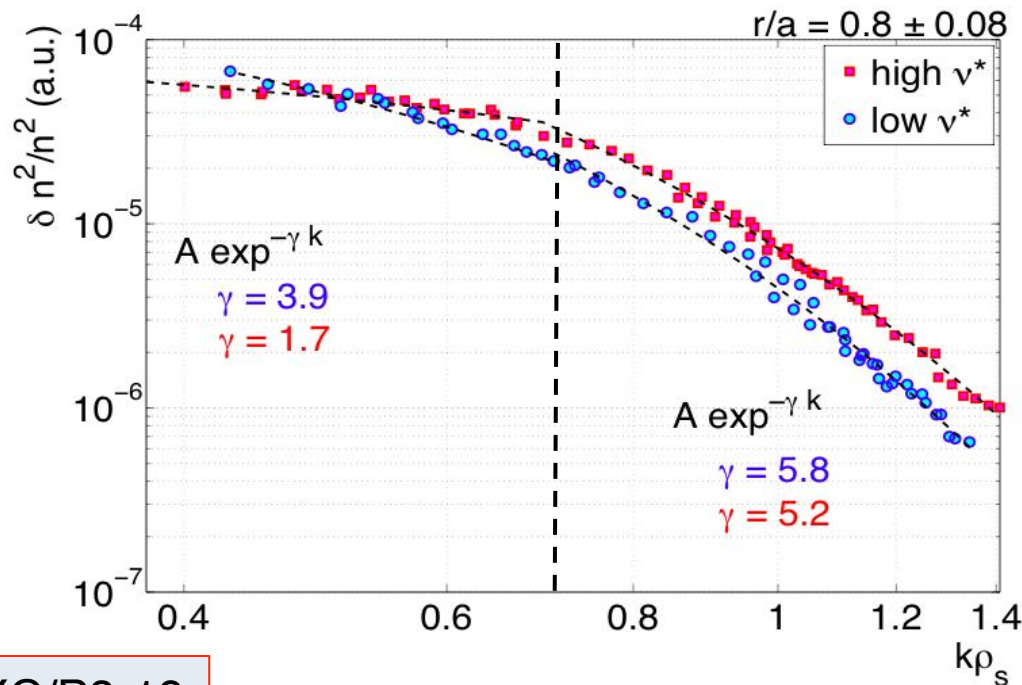
<i>Topical Area:</i>	<i>Number of Papers</i>
Innovative Confinement Concepts	10
Operational Scenarios	28
– Stellarators	
– Elmy H-modes	
– Advanced Operating Modes	
✓ Confinement Experiments	51
– <i>Energy Transport and Turbulence</i>	
– <i>Particle Transport</i>	
– <i>Rotation and Momentum Transport</i>	
– <i>L-H transition and Pedestal</i>	

Subtle Differences in Electron Transport and NBI Sources Lead to Different Reversed Shear States in JET and JT-60U

- **Good match in dimensionless parameters except:**
 - Mach number
 - Differences in v^* and β due to density profile.
- **Density profile peakedness in JT-60U enables a higher bootstrap current fraction.**
- ***Need good predictive model to extrapolate to ITER.***



Influence of Collisionality on Turbulence Spectra Studied in Tore Supra



L. Vermare, EXC/P8-19

- Dimensionless scans were conducted to determine the effect of ν^*
- Does not support standard explanation on effect of ν^* on zonal flows.

Experimental Test of Predicted Turbulence Amplitudes and Cross-Phases Conducted in the Core

As T_e/T_i increases with the addition of ECH to an NBI heated L-mode...

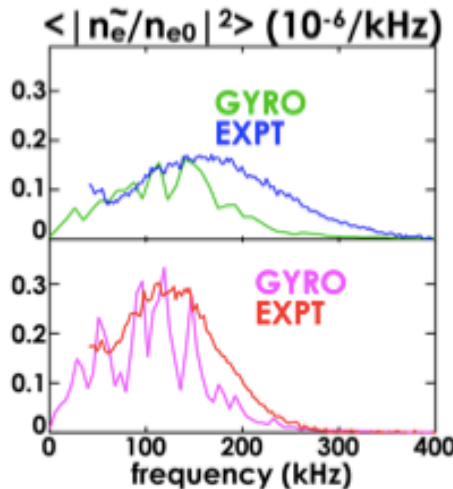
DIII-D

$\rho=0.6$

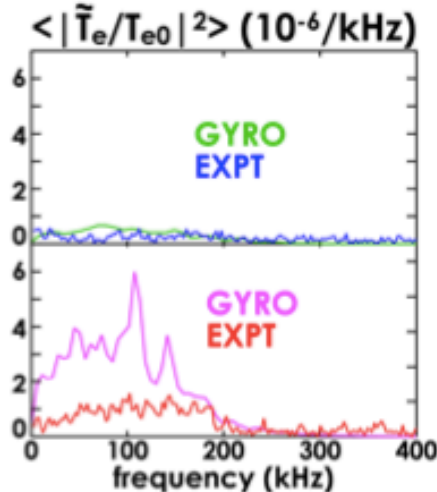
NBI only
 $T_e \approx T_i$

NBI+ECH
 $T_e > T_i$

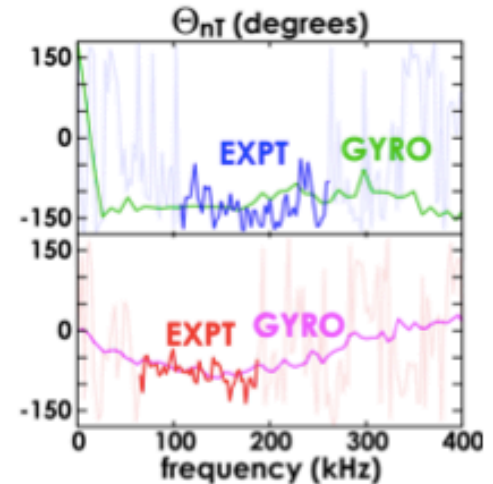
- Change in \tilde{n} in agreement with GYRO



- GYRO over-predicts observed increase in \tilde{T}_e



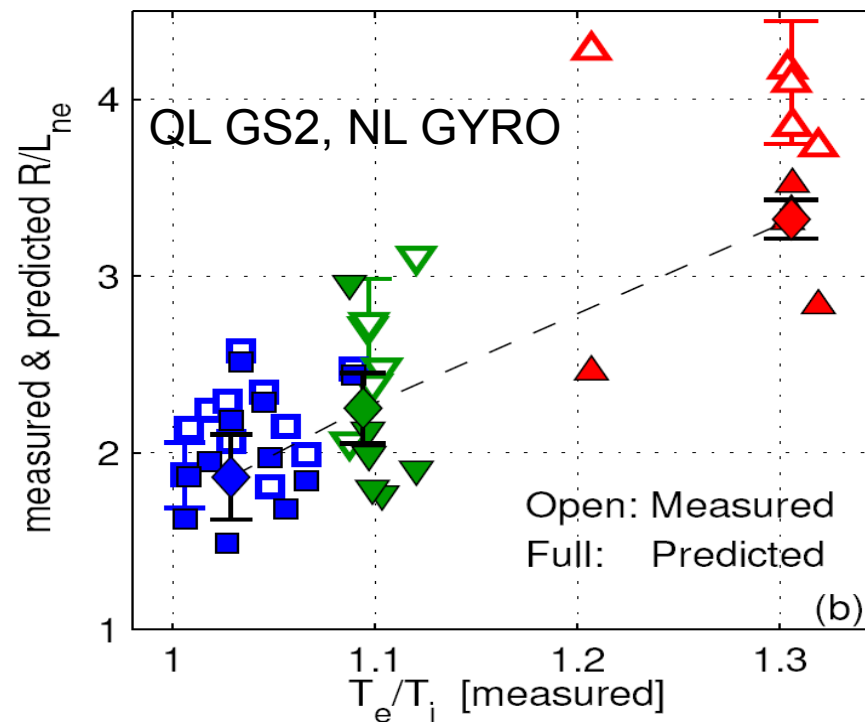
- Change in n-T cross phase as predicted by GYRO



T. L. Rhodes, EXC/7-2

- GYRO reproduces many features in the core but not in the edge ($\rho > 0.75$) or the core of L-mode discharges.
 - Experiments used to establish the range of validity of the codes.

Density Profile Peaking is Reproduced by Gyrokinetic Modelling (at $r/a=0.5$)



AUG

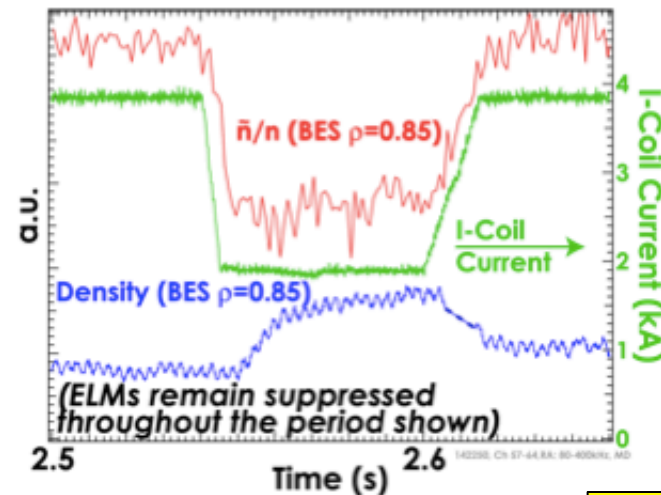
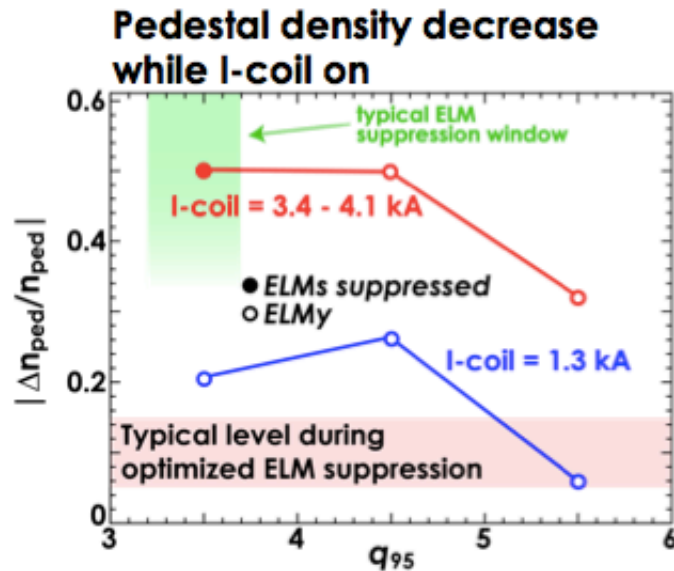
A. Kallenbach,
EXC/OV3-1

- Central density increases with the application of ECH to NBI heated plasmas.
 - Flattens the ion temperature and rotation profile
- In simulations the measured profiles are used as input.
- Results are sensitive to input parameters (e.g. T_e/T_i , R/L_{Te} , ν_{ei})

Initial DIII-D Measurements Near Top of the Pedestal Indicate Non-axisymmetric Fields Modify Density Turbulence

- Density decrease observed over a range of q_{95}

- Particle transport correlated with increased fluctuations at higher I-coil current

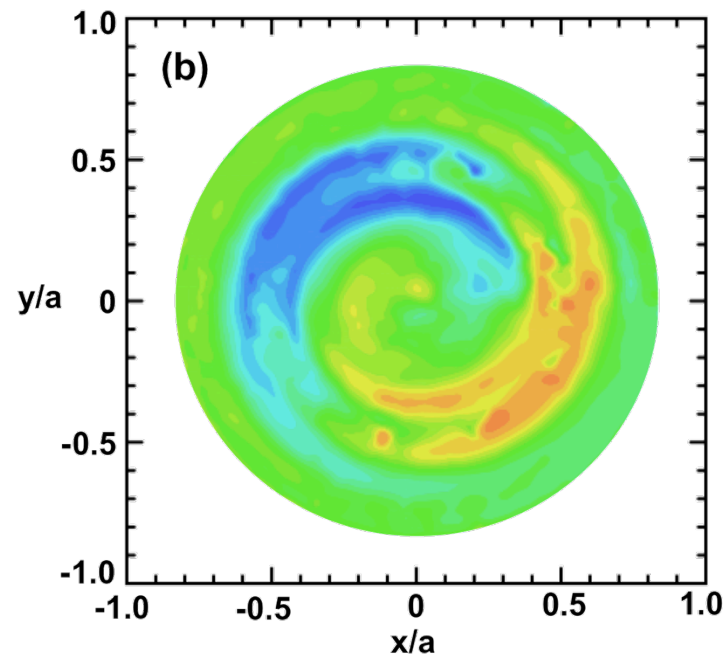


Z. Yan, EXC/P3-05

DIII-D

- Increased particle transport also occurs outside of ELM suppression window.

Long Coherence Length Temperature Fluctuations Found in LHD



S. Inagaki, EXC/7-4

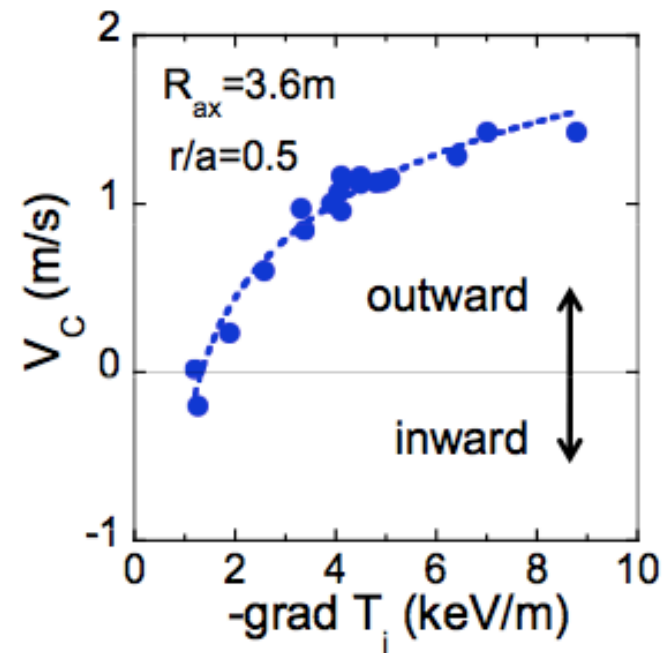
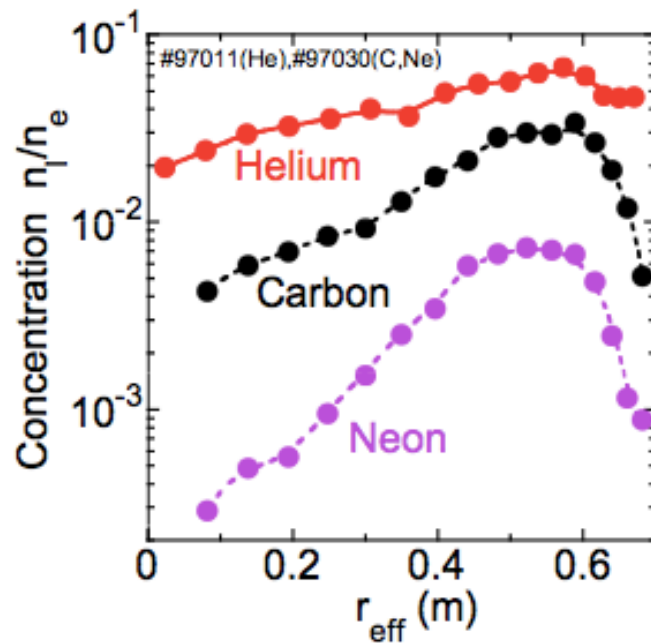
Radial correlation length $\sim a$

Ballistic transport from core to the edge inferred

Impact of long-range fluctuations on transient particle transport was studied.

Is this the long sought explanation for cold pulse propagation or non-local transport?

“Impurity Holes” Observed in LHD in Discharges with Large T_i Gradients

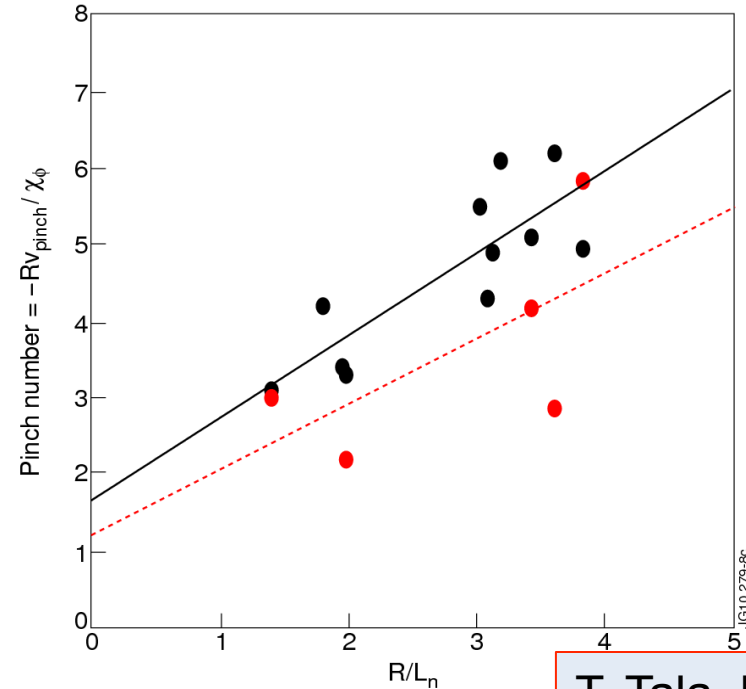
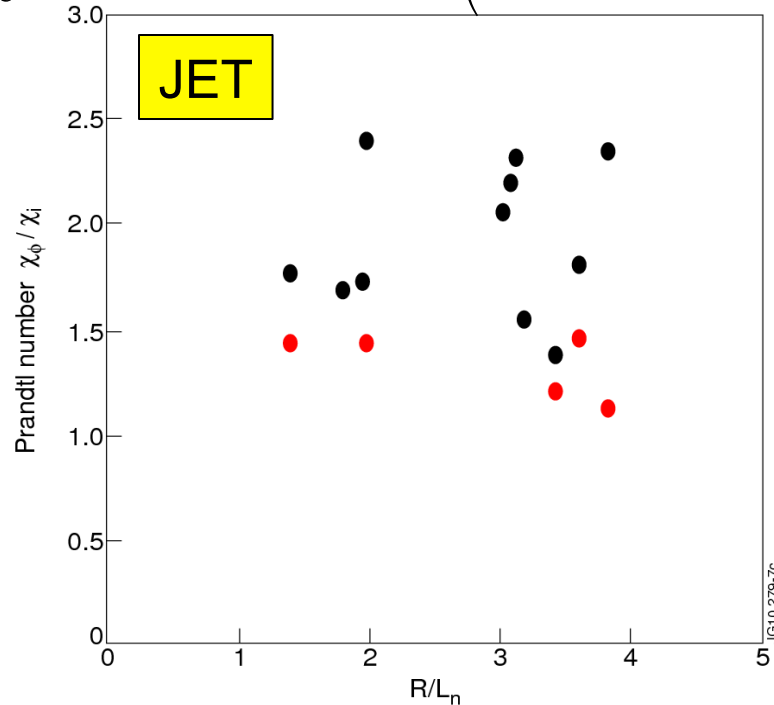


M. Yoshinuma, EXC/9-1

- Large anomalous outward convective impurity transport inferred.
 - In spite of negative E_r

Momentum Transport Studies Show No Dependence on Collisionality of Either Prandtl or Pinch Numbers

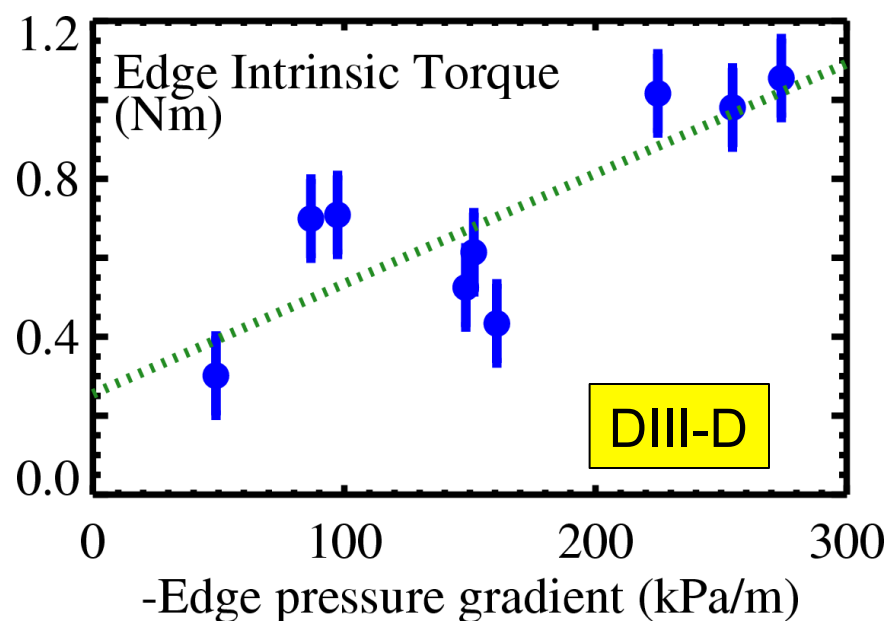
$$\underbrace{mR \frac{\partial n V_\phi}{\partial t}}_{\text{Rate of change of angular momentum}} = \underbrace{\sum \eta}_{\text{Input torque}} - \nabla \cdot \left(\underbrace{-mnR \left(\chi_\phi \frac{\partial V_\phi}{\partial r} - V_\phi V_{pinch} \right)}_{\substack{\text{diffusion} \\ \text{pinch}}} + \underbrace{\Pi_{RS}}_{\substack{\text{Residual stress} \\ \text{"Intrinsic source"}}} \right) - \underbrace{\frac{mnR(V_\phi - V_\phi^*)}{\tau_{damp}}}_{\text{Neoclassical viscous drag}} + \underbrace{\langle \tilde{J} \times \tilde{B} \rangle}_{\text{Maxwell stress}} + \dots$$



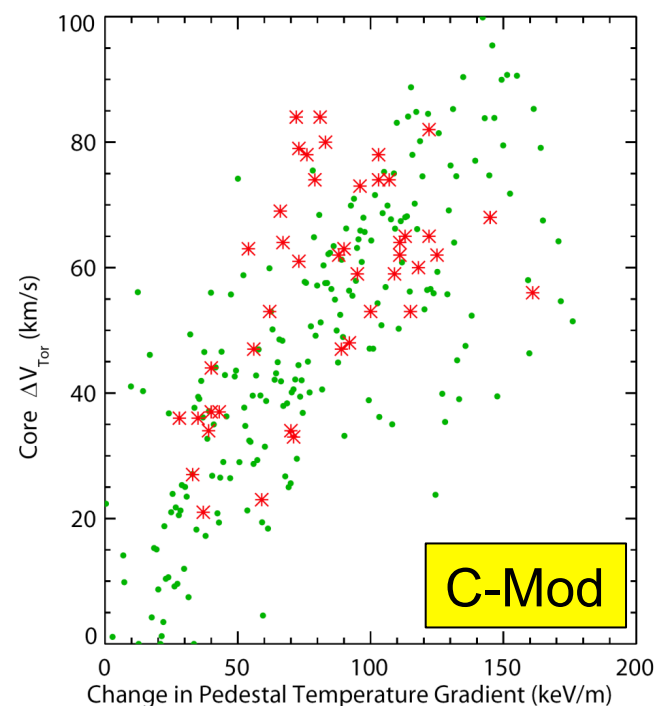
T. Tala, EXC/3-1

JET experimental data is compared with GS2 calculations in red.

Edge Intrinsic Rotation Appears to Be Driven by Pedestal Gradients



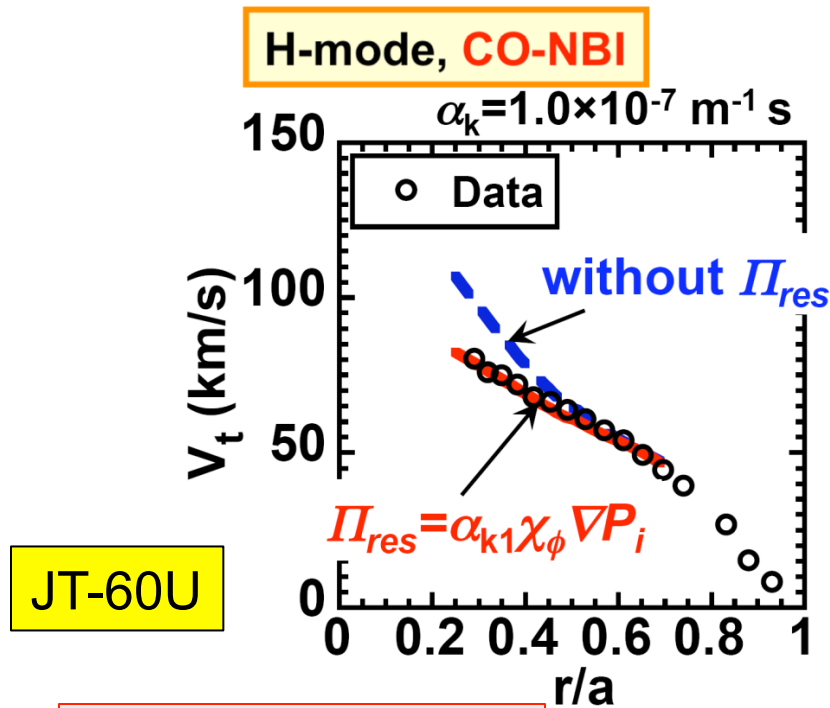
W. Solomon, EXC/3-5



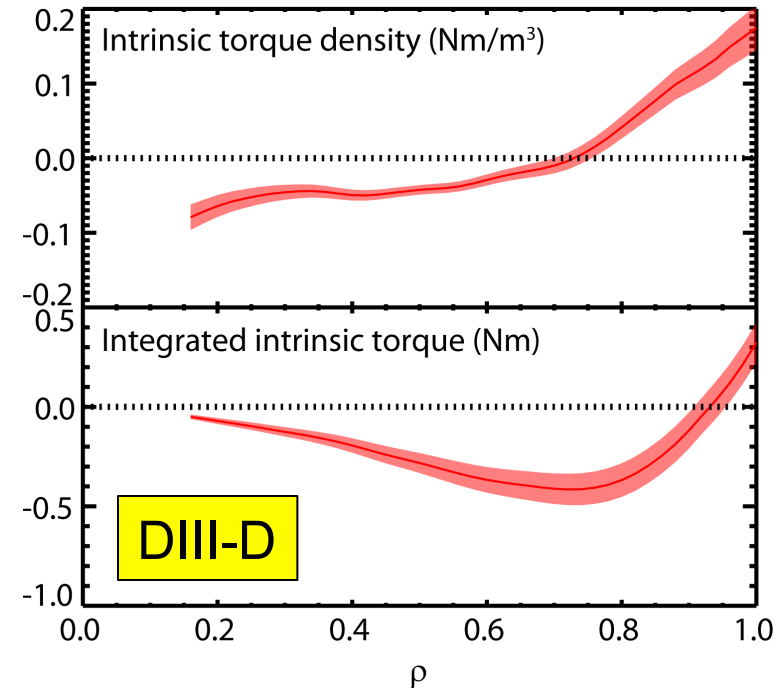
J. Rice, EXC/3-3

- Suggestive that turbulent residual stress may be key in generating intrinsic rotation (DIII-D, C-Mod, LHD, JT-60U, ...)
- Reynolds stress sufficient to account for intrinsic rotation in CSDX at UCSD, but not on DIII-D.

Intrinsic Drive in the Core Can Also Influence Rotation Shear



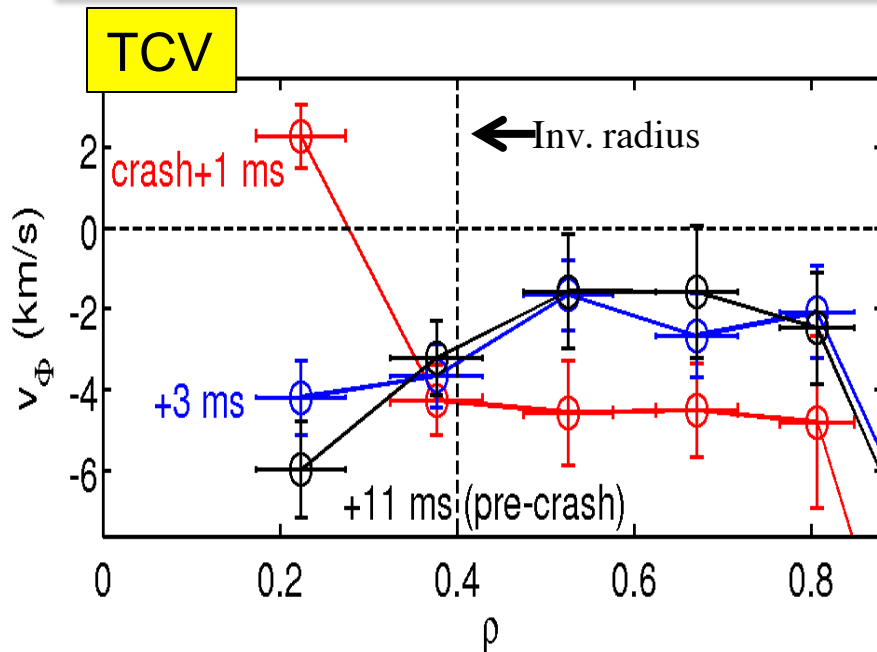
M. Yoshida, EXC/3-2



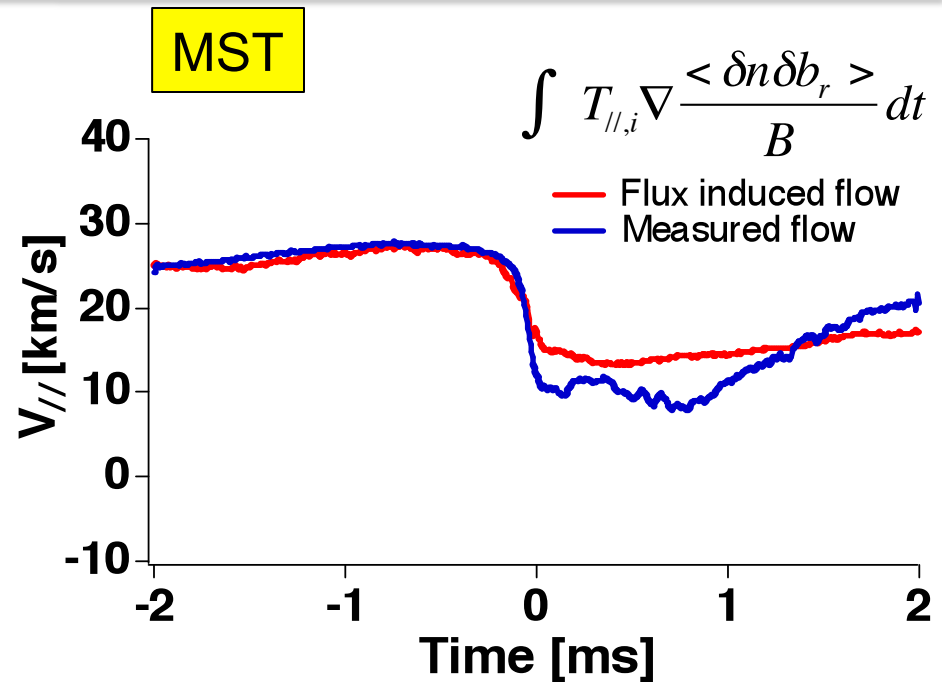
W. Solomon, EXC/3-5

- ITBs with strong pressure gradients (JT-60U)
- Other residual stress drive, including effect of ECH observed on DIII-D.

Core MHD Can Also Modify Rotation Profile



B. P. Duval, EXS/P4-01



D. Brower, EXC/P4-02

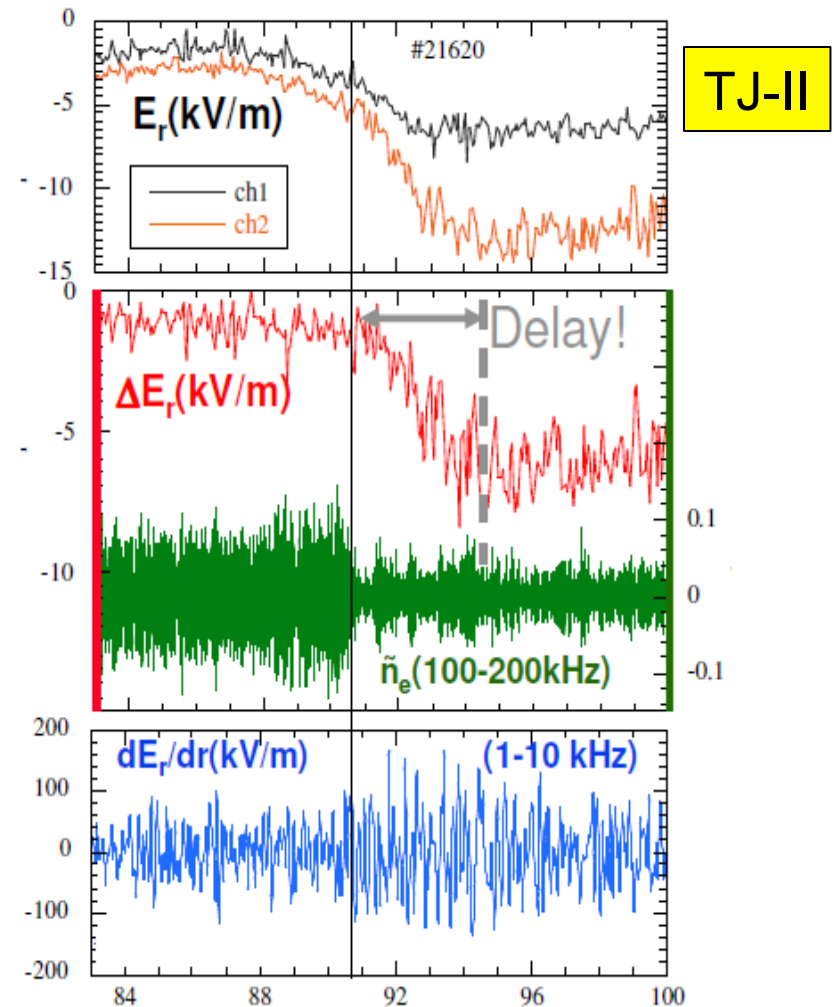
- Rotation profile in TCV modified by sawteeth crash.
- Detailed measurements of Maxwell stress in MST following a sawtooth event in agreement with flux induced flow.
- *Extrapolation to ITER remains to be established.*

Role of Fluctuating Sheared Flows in L-H Transition Is Identified to Be Important

The L-H transition appears more correlated with the development of fluctuating flows than mean shear E_r effects

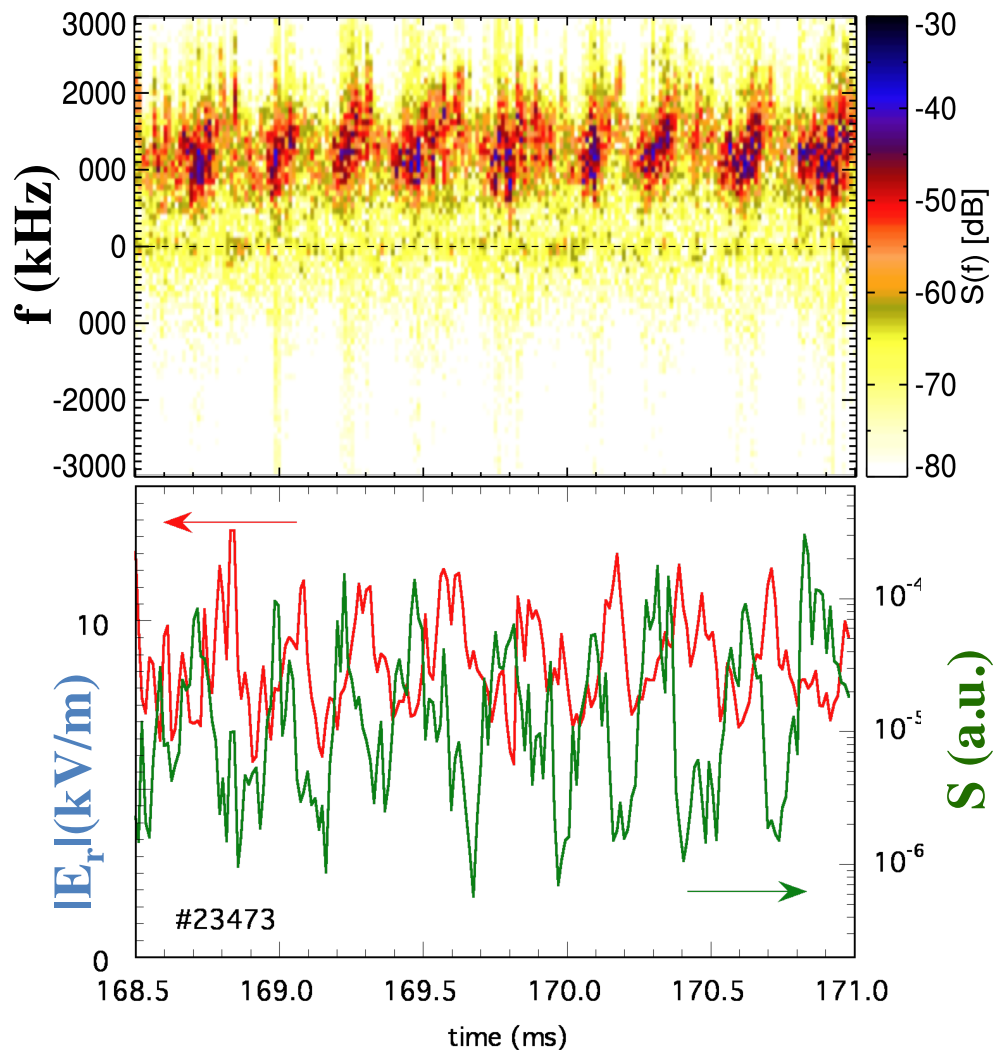
- TJ-II as well as MAST (H. Meyer, EXC/2-3Ra) and NSTX (S. Kaye, EXC/2-3Rb) reported no significant change in mean shear prior to transition.

Doppler reflectometry enables local measurements of oscillating radial flows.

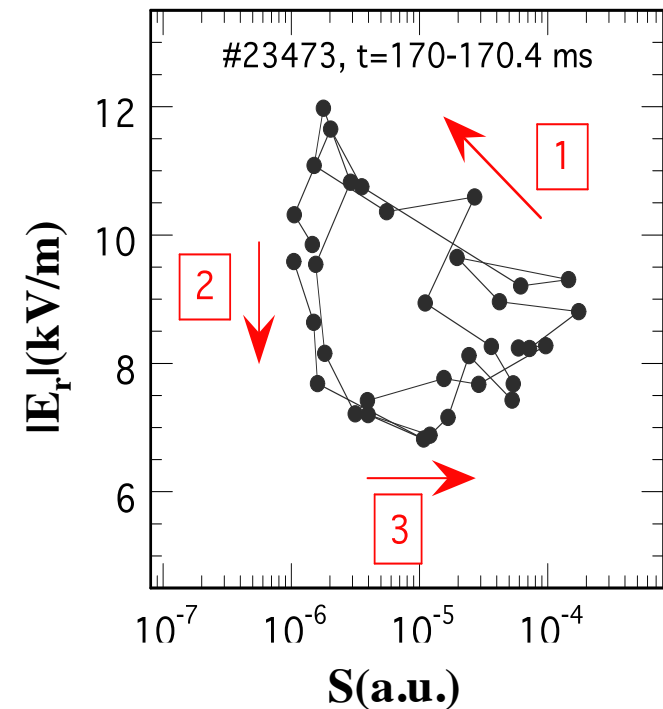


T. Estrada, EXC/P3-01

Time Evolution of Flows and Turbulence in a Slow Transition to H-Mode Indicates a Predator-Prey Behavior



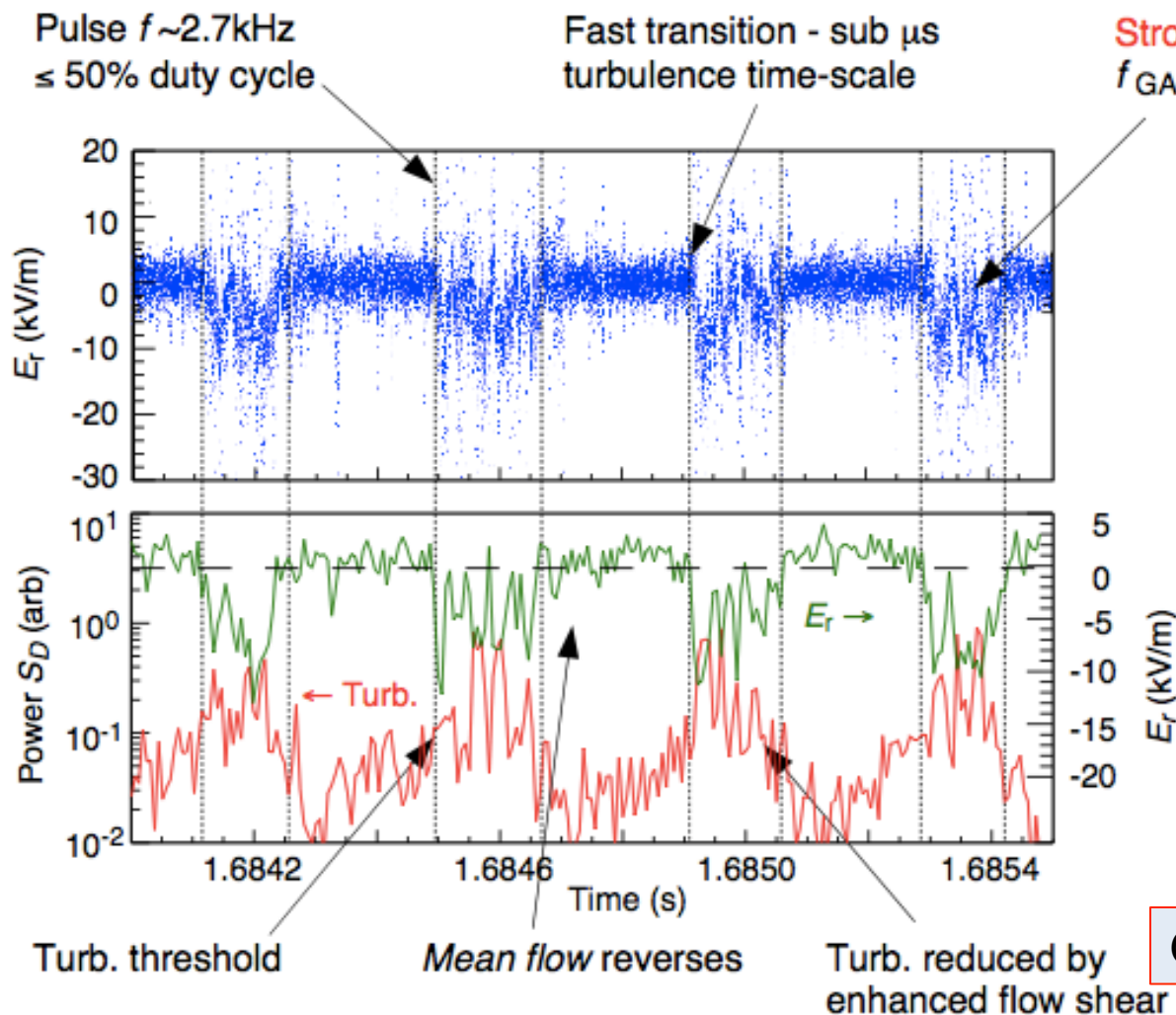
TJ-II



Is this a high frequency dithering H-mode?

Are GAM's the Missing Link During the Intermediate Phase Prior to Transition to H-mode?

AUG



- Doppler $f_D = d\phi/dt$
 (50ns resolution)
- Turbulence threshold
 \rightarrow Drives flow & GAM
 \rightarrow Shear erodes turb.
- Limit-cycle behaviour
- GAM E_r shearing rate
 $>$ turb. de-correlation τ_c
- Equilibrium time scale:
 I-phase supports larger edge $\nabla P \rightarrow$ mean flow

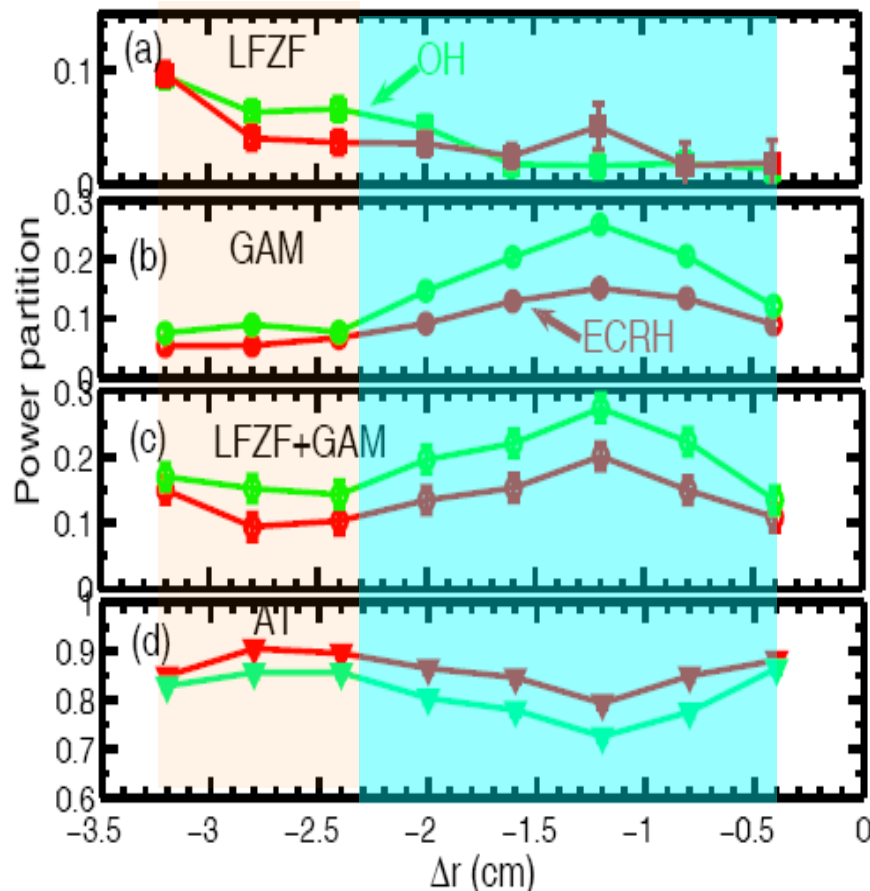
G. D. Conway, EXC/7-1

- Is the AUG I(ntermediate)-phase related to the C-Mod I-mode?

What Are the Role of Zonal Flows?

HL-2A

Coexistence GAM dominant



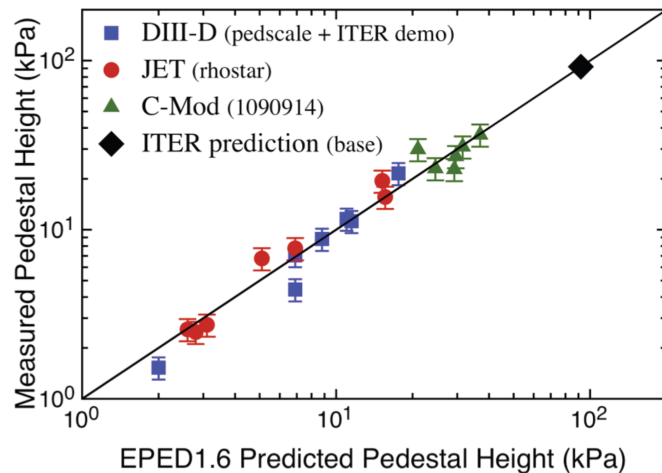
K. J. Zhao, EXC/7-3

Probe measurements in the edge (near LCFS) of HL-2A indicate that GAMs are dominant

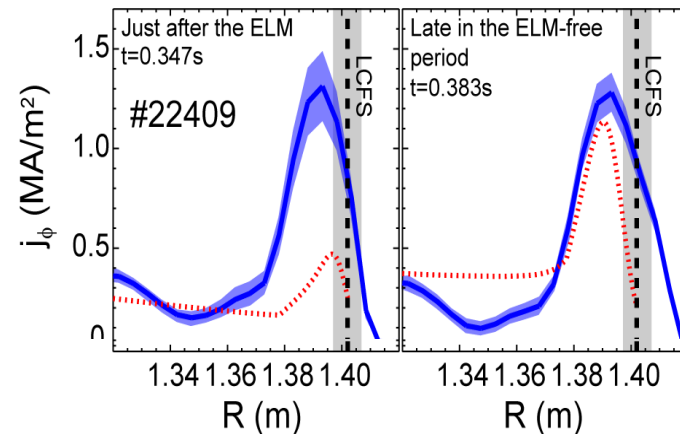
- Further inside GAMs and Zonal Flows coexist.
- Also see Y. Xu, EXC/9-3

To fully understand the dynamics of the turbulence in the edge leading to an L to H transition would want to measure the spatial evolution of turbulent structures.

Detailed tests of EPED Model and Peeling/Ballooning Paradigm in Progress



P. Snyder, THS/1-1

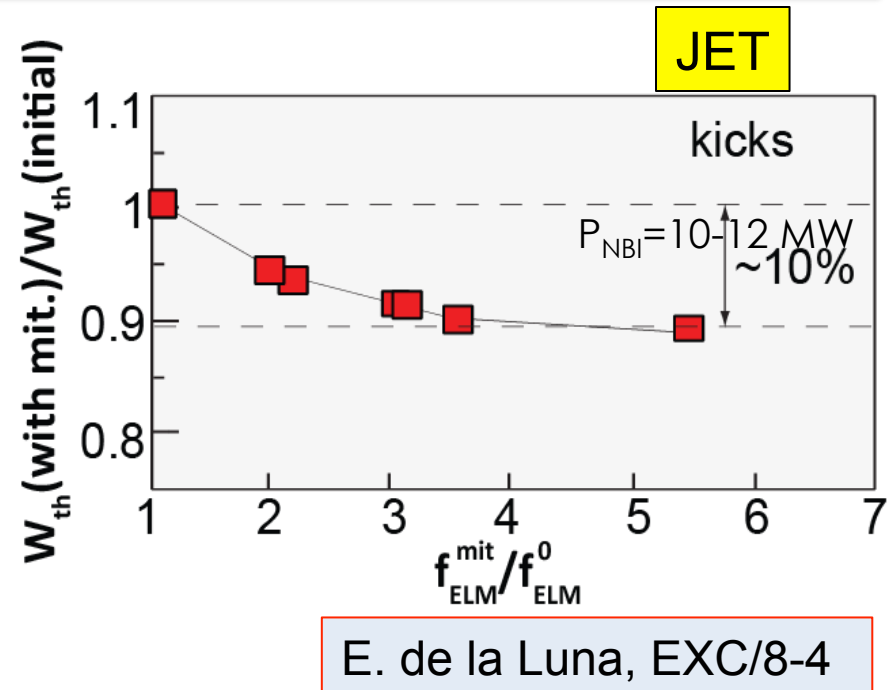
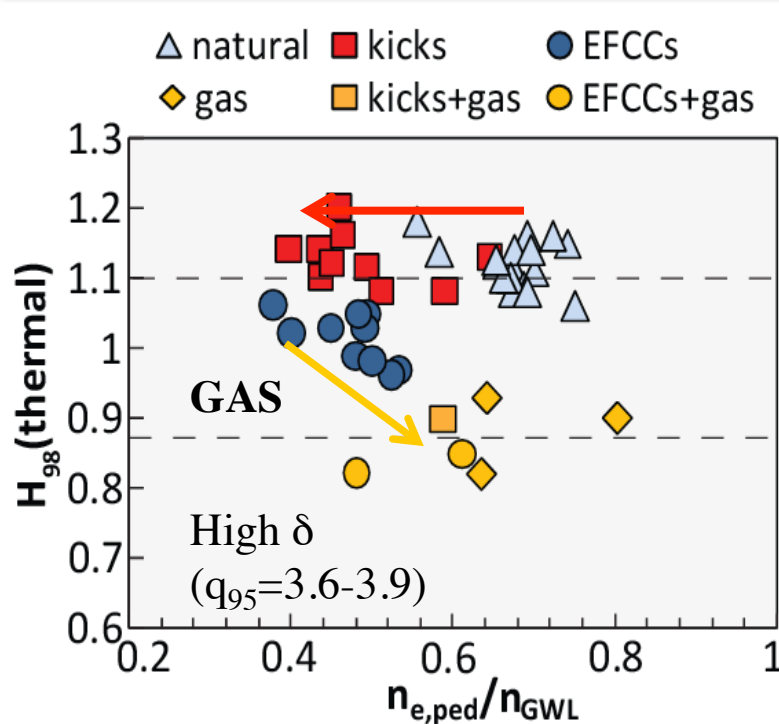


MAST

H. Meyer EXC/2-3a

- **EPED 1.6 works well for range of devices**
 - High frequency coherent modes during QH-mode looks like KBM in DIII-D (Z. Yan, EXC/P3-5)
- **Pressure gradients saturate at least $\frac{1}{2}$ way thru ELM cycle in AUG**
 - edge current diffusion calculations suggest j_{BS} equilibrates rapidly
 - What kicks off the next ELM? (B. Kurzan, EXC/P3-3)
- **MAST plasma can stay above ballooning boundary for ~ 10 ms before ELM**
 - New MSE measurements of bootstrap current compared with neoclassical model

ELM Mitigation Results in Loss of Density and/or Confinement

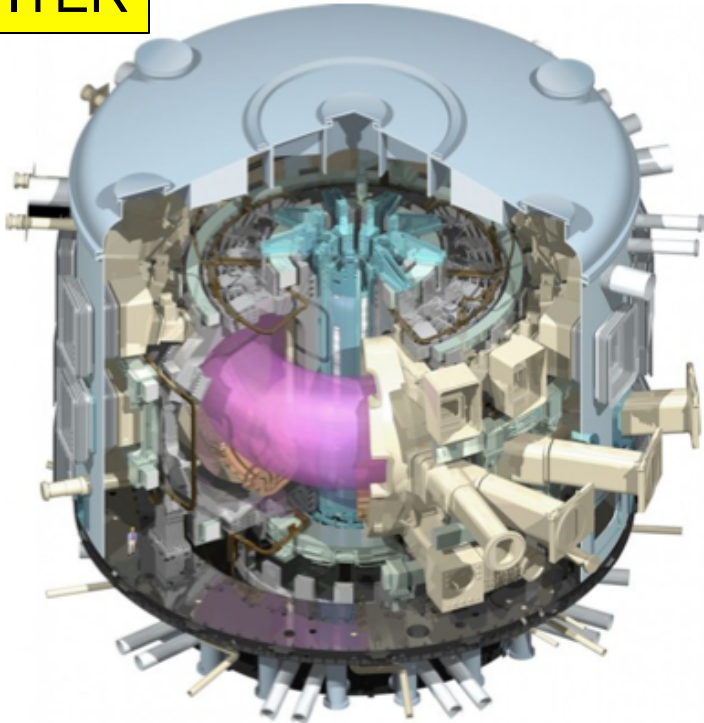


E. de la Luna, EXC/8-4

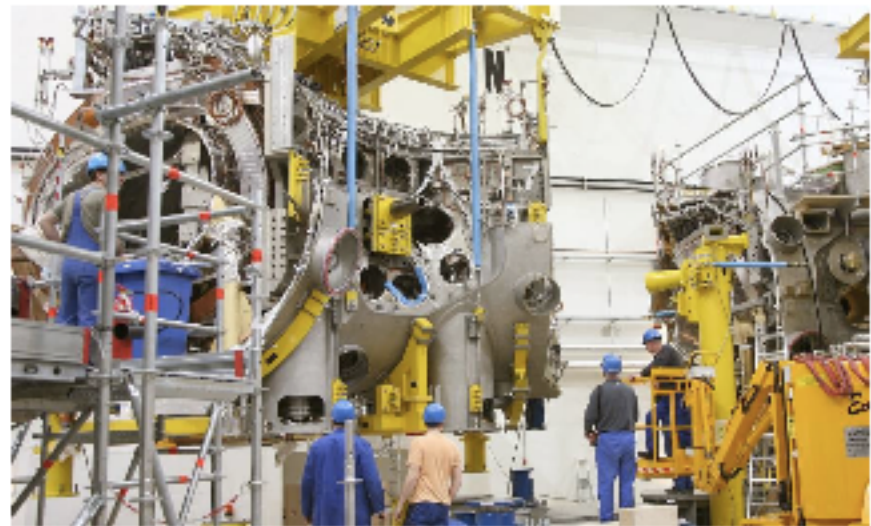
- Good confinement during ELM mitigation (unfuelled) $\rightarrow H_{98} \sim 1.1$ but density reduced by 20%
- Density can be restored by gas fuelling but confinement decreases.
- *Ultimately may have to reduce ITER performance to avoid ELM damage to divertor tiles.*

Congratulations on Excellent Progress!

ITER



W7-X



Results presented at the 23rd FEC meeting are significant contributions to the success of ITER and W7-X.